

A Study on Fracture Surface of Aged Turbine Rotor Steel by Fractal Dimension

Amkee Kim*

Department of Mechanical Engineering, Kongju National University, Chungnam 314-701, Korea

Seung Hoon Nahm

Korea Research Institute of Standards and Science Taejon 305-600, Korea

Since fracture surface presents clear evidence to describe the circumstances of material failure event, analysis of fracture surface should provide plenty of useful information for failure prevention. Thus if we extract proper information from the fracture surface, the safety evaluation for plant component could be more accurate. In general, the chaotic morphology of fracture surface is determined by the degree of material degradation as well as by other factors such as type of load, geometry of specimen, notch condition, microstructure of material and environment. In this research, we developed a fractal analysis technology for the fracture surface of aged turbine rotor steel based on the slit-island technique using an image analyzer. Moreover the correlation between the fractal dimension and the aging time was studied.

Key Words : Fractal Dimension, Fracture Surface, Charpy Impact Test, 1Cr-1Mo-0.25V Steel, Material Degradation, Image Analyzer

1. Introduction

If equipment serves for a long period of time, its material suffers aging, and thus its properties change gradually. One of main factors of equipment aging is material degradation. Material degradation takes place because of the long exposure to elevated temperature, corrosive environment etc. combined with loading (Shoji and Takahashi, 1987; Schwant and Timo, 1985; Nahm et al., 1998). Particularly, the turbine rotor steel degradation is caused by the micro-structural change such as precipitation of carbide and decrease of solid element within matrix, and the distribution of macroscopic defects such as void or crack (Abdel-Latif et al., 1982). One well known evaluation technique for the toughness degradation of turbine rotor steel is to use FATT

(Fracture Appearance Transition Temperature) which is very closely related with the morphology of fracture surface (Coster and Chermant, 1983; Underwood and Banerji., 1986; Saouma et al., 1990; Mandelbrot et al., 1984; Tanaka, 1993; Williford, 1988; Wang et al., 1988). It implies that the quantification of fracture surface may provide useful information regarding turbine rotor degradation.

Since, at present, fractal analysis might be the most adequate tool for the characterization of such chaotic morphology as fracture surface, we developed a fractal analysis technology for the fracture surface of aged turbine rotor steel based on the slit-island technique using an image analyzer in this research. Charpy specimens with six different aging periods were artificially prepared by an isothermal heat treatment at 630 °C, and tested at different temperatures. In addition, fractal analysis on the fracture surfaces of Charpy impact specimens was carried out, and the correlation between the obtained fractal dimension and the aging time was established.

* Corresponding Author,

E-mail : amkee@kongju.ac.kr

TEL : +82-41-850-8616; FAX : +82-41-854-1449

Department of Mechanical Engineering, Kongju National University, Chungnam 314-701, Korea. (Manuscript Received April 16, 2001; Revised July 25, 2001)

Table 1 Chemical compositions (wt. %)

Element	C	Si	Mn	P	S	Sb	
Composition	0.31	0.29	0.80	0.015	0.022	0.015	
N	Cu	Ni	Cr	Mo	V	Sn	As
0.013	0.21	0.39	1.19	1.42	0.25	0.004	0.015

Table 2 Mechanical properties

Temp. (°C)	Yield Strength (MPa)	Tensile Strength (MPa)	Elongation (%)	Reduction of Area (%)
24	665.2	823.1	18.8	59.4
538	533.5	580.6	22.7	55.5

2. Experiments

2.1 Material and specimen

The test material is 1Cr-1Mo-0.25V steel which is widely used as a steam turbine rotor material. The chemical compositions and the mechanical properties are contained in Table 1 and Table 2 respectively.

Virgin materials (as received) were artificially aged by the isothermal heat treatment of 630 °C for 0, 670, 1340, 1832, 3640 hours, which is the accelerating aging process for simulating the microstructures of materials served at steam temperature of 538 °C for 0, 4, 8, 12, 23 years respectively. The heat treatment times for the simulation were selected based on Arrhenius self-diffusion theory of the iron element (Fe) (Abdel-Latif et al., 1982). Five kinds of specimens with different aging periods were prepared. 55×10×10 (mm) ASTM standard V notched Charpy impact specimens were machined and tested (ASTM E23, 1997). The notch direction is parallel to the rolling direction. The notch depth is 2 mm, and the radius of notch root is 0.25 mm. Impact tests were carried out at 24, 75, 115, 160 °C.

2.2 Measurement of fractal dimension of fracture surface

Fractured specimens, obtained from the impact test, were carefully cleaned and coated with nickel as shown in Fig. 1(b). The nickel coating

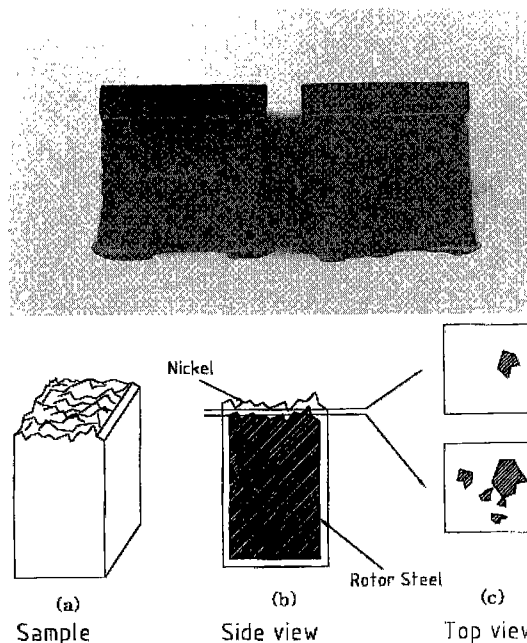


Fig. 1 Fractured specimen is encapsulated in epoxy and polished parallel to the fracture plane. Islands emerge in the polished plane

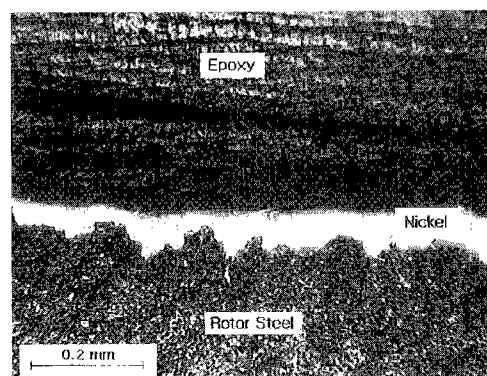


Fig. 2 A profile of fracture surface from the cross section

performs two functions: It provides good contrast during observation, and helps to preserve the fracture surface during the polishing.

Figure 2 represents a profile of fracture surface from the cross section etched by 5 % nital (HNO_3 +methyl alcohol) solution. The coated samples were mounted in epoxy and polished parallel to the fracture surfaces as depicted in Fig. 1 (b) and (c). As the fracture surface is

encountered, a section of the fracture surface appears in the polished plane as shown in Fig. 1 (c). These sections appear as islands (so-called slit-island) in the polishing plane. As the polishing proceeds, these islands begin to grow. The perimeter of the island (see Fig. 3) presents a curved line that can be measured according to

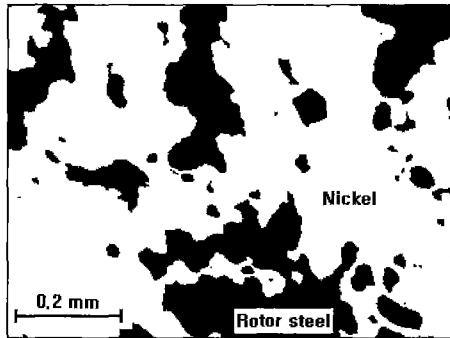


Fig. 3 Appearance of islands on polished surface

Richardson's equation. An adaptation of Richardson's equation reveals a relationship (Mandelbrot et al., 1984; Kim et al., 1999) between area and perimeter of an island:

$$P \propto A^{D/2} \quad (1)$$

Where A is the island area, P is the island perimeter and D is the fractal dimension of the perimeter. Areas and perimeters of islands at the central region of fracture surface are measured by using the image analyzer attached to an optical microscope. Figure 3 represents an image of islands on a polished plane.

3. Results and Discussion

3.1 Impact energy and fracture surface

Figure 4 represents the variation of impact energy with the test temperature. The solid line

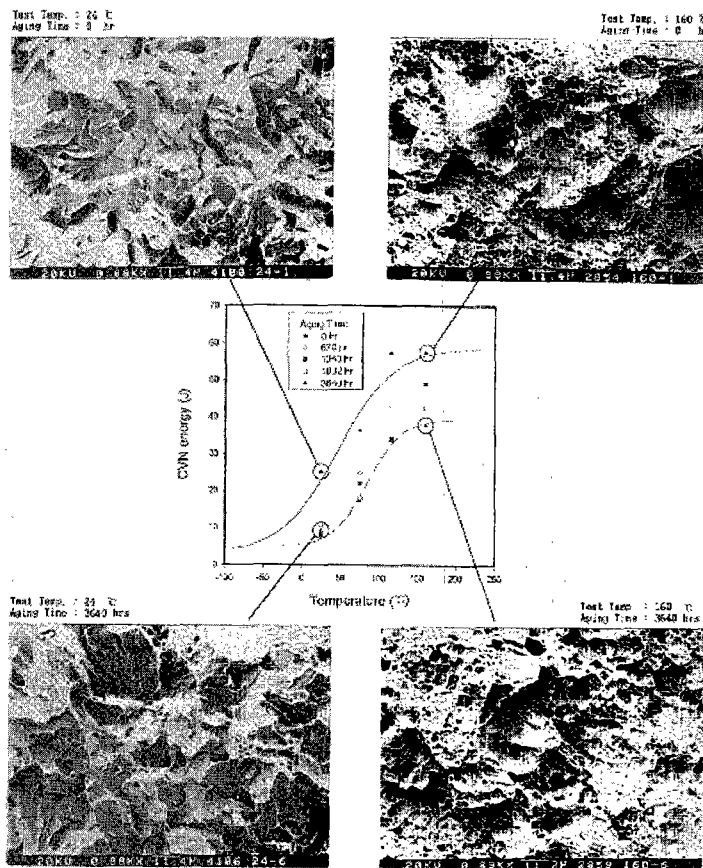


Fig. 4 Fracture surface appearance of Charpy impact specimens

and the broken line represent the regression lines for 0 hour aged (virgin) material and 3640 hours aged material respectively. Equation (2) was utilized for the regression lines.

$$CVN \text{ energy} = A + B \tanh\left(\frac{T - T_0}{C}\right) \quad (2)$$

Here, fitting constants A, B, T_0 , C for 0 hour aged material are 33.1 J, 31.6 J, 52.8 °C, 88.7 °C, and those for 3640 hours aged material are 22.2 J, 17.2 J, 84.1 °C, 43.8 °C. Most of data for materials between 0 and 3640 hours are distributed inside of those two fitting lines. The impact energy appears the lower in case of the more aged material within materials tested at the same temperature. The upper shelf energy decreases with the increment of aging time, and the ductile brittle transition temperature corresponding to 1/2 the sum of upper shelf energy and lower shelf energy increases with the increment of aging time.

SEM (scanning electron microscopy) fractography in Fig. 4 indicates that the ductile fracture surface full of dimples appears above the transition temperature while the macroscopically brittle fracture surface appears below the transition temperature. However, it seems almost impossible to distinguish between the extents of degradation of materials by using such qualitative means as SEM. Thus the more sophisticated quantification technology of fracture surface should be attempted.

3.2 Variation of fractal dimension of fracture surface with aging time

Figure 5 represents a typical example of the relationship between perimeter P and area A in logarithmic scale. Since the slope of linear regression line represents $D/2$ of Eq. (1), the fractal dimension of 0 hour aged material tested at room temperature (24 °C) is 1.29. Following the same procedure allows one to obtain the rest of fractal dimensions regarding all the tested fracture surfaces. Figure 6 represents the fractal dimension variation of fracture surfaces tested at 24 °C with the aging time and the FATT. The fractal dimension decreases monotonously with aging time while the FATT increases. The variation of

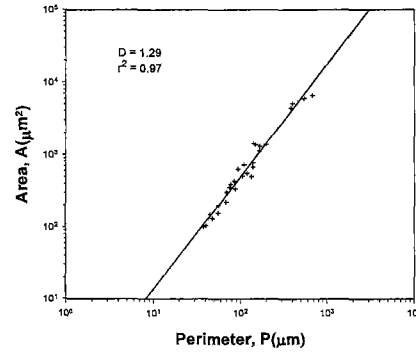


Fig. 5 Relationship between perimeter and area of slit-island for non aged specimen tested at 24 °C

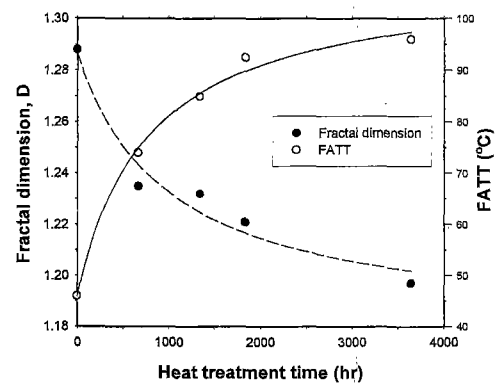


Fig. 6 Variation of fractal dimension and FATT with aging time

fractal dimension and FATT would be caused by the change of microstructure of 1Cr-1Mo-0.25V steel with aging time. Indeed, Figure 7 represents the EPMA (electron probe micro analyzer) area map which shows carbides formed at grain boundary of aged 1Cr-1Mo-0.25V steel by carbon which was moved from matrix. The amounts of Cr, Mn, Mo and C at the grain boundary increase as the aging time increases (Ryu et al., 2000). The precipitation of carbides reduces the strength of grain boundary because of their brittleness as well as softens the matrix with the decreased amount of carbon compound in the matrix. Consequently, it might change the morphology of fracture surface of material with aging time.

Figure 8 represents a good linear relationship between the fractal dimension and the FATT.

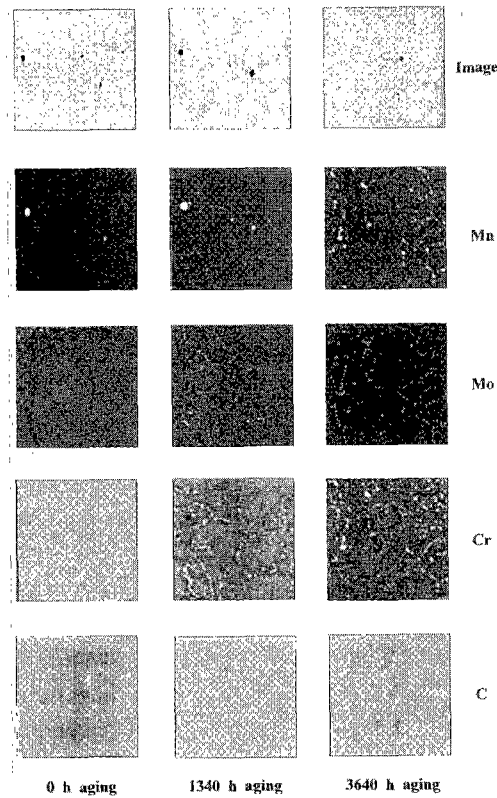


Fig. 7 Change of EPMA area mapping with aging time

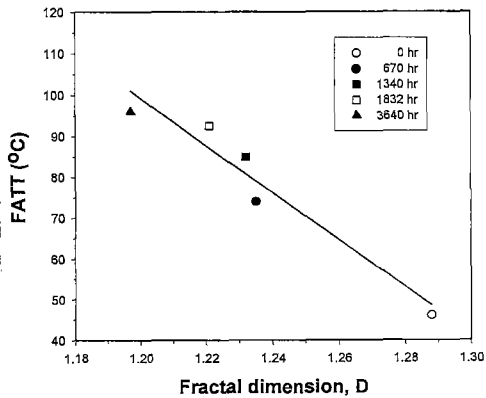


Fig. 8 Relationship between fractal dimension and FATT

Thus the linear relationship can be utilized to estimate the extent of toughness degradation due to aging by the fractal dimension of fracture surface.

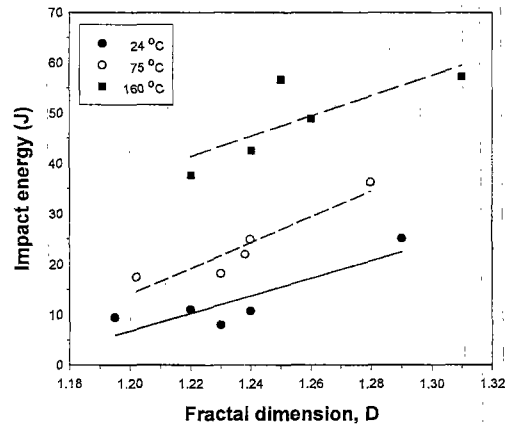


Fig. 9 Fractal dimension versus Charpy impact energy at various test temperatures

3.3 Relationship between fractal dimension and impact energy

Figure 9 represents the correlations between fractal dimension and Charpy impact energy at various test temperatures. The Charpy impact energy turns out to be linearly correlated with the fractal dimension within materials tested at same temperature. It implies that fracture properties of material such as impact energy (or fracture toughness) may be also evaluated simply by the fractal analysis on fracture surface. The further study of relationships between the fracture properties and the fractal dimension of fracture surface would provide beneficial information for the prediction of material properties using the fracture surface analysis, and thus remains as a future work of this study.

4. Conclusions

The fractal dimensions of fracture surfaces of artificially aged turbine rotor steel were studied based on the slit-island technique using an image analyzer in this study. The obtained results are summarized as follows:

- (1) The fractal dimension of fracture surface decreases monotonously with the increment of aging time. The fractal dimension of fracture surface tested at room temperature has a good linear relationship with FATT. Thus it allows one to estimate the extent of toughness degrada-

tion due to aging based on the fractal dimension analysis of fracture surface.

(2) Charpy impact energy is linearly correlated with the fractal dimension within materials tested at same temperature. Thus fracture properties such as impact energy may be dependent on not only the change of macroscopic properties, i. e., softening, but also the geometrical morphology of fracture surface determined by the micro-structural heterogeneity of material depending on aging.

References

- Abdel-Latif, A. M., Corbett, J. M. and Taplin, D. M. R., 1982, "Analysis of Carbides Formed During Accelerated Aging of 2.25Cr-1Mo Steel," *Metal Science*, Vol. 16, pp. 90~96.
- ASTM Standard E23, 1997, "Notched Bar Impact Testing of Metallic Materials," ASTM Philadelphia.
- Coster, M. and Chermant, J. L., 1983, "Recent developments in quantitative fractography," *International Metals Reviews*, Vol. 28, No. 1, pp. 228~250.
- Kim, A., Nahm, S. H. and Kim, J. K., 1999, "Fractal Dimension Analysis on Fracture Surface of Degraded Turbine Rotor Steel by Slit-island Technique," *Transactions of the KSME (A)*, Vol. 23, No. 1, pp. 47~56.
- Mandelbrot, B. B., Passoja, D. E. and Paullay, A. J., 1984, "Fractal Character of Fracture Surfaces of Metals," *Nature*, Vol. 308, No. 19, pp. 721~722.
- Nahm, S. H., Kim, A. and Yu, K. M., 1998, "Nondestructive Evaluation of Toughness Degradation of 1Cr-1Mo-0.25V Steel Electrical Resistivity," *Transactions of the KSME (A)*, Vol. 22, No. 5, pp. 814~820.
- Ryu, K. S., Nahm, S. H., Kim, Y. I., Yu, K. M., and Son, D., 2000, "Degradation Evaluation in Aged 1Cr-1Mo-0.25V Steel Using Magnetic Permeability," *Journal of Materials Science Letters*, Vol. 19, pp. 1759~1761.
- Saouma, V. E., Barton, C. C. and Gamaleldin, N. A., 1990, "Fractal Characterization of Fracture Surfaces in Concrete," *Engineering Fracture Mechanics*, Vol. 35, pp. 47~53.
- Schwant, R. C. and Timo D. P., 1985, *Life Assessment and Improvement of Turbogenerator Rotors for Fossil Plants*, New York, Pergamon Press, pp. 325~340.
- Shoji, T. and Takahashi, H., 1987, "Life extension and assessment of Fossil Power Plants," *EPRI CS-5208, Electric Power Research Institute*, Palo Alto, California, pp. 745~759.
- Tanaka, M., 1993, "The Fractal Dimension of Grain Boundary Fracture in High Temperature Creep of Heat Resistant Alloys," *Journal of Material Science*, Vol. 28, pp. 5753~5758.
- Underwood, E. E. and Banerji, K., 1986, "Fractals in Fractography," *Materials Science and Engineering*, Vol. 80, pp. 1~14.
- Wang, Z. G., Chen, D. L., Jiang, X. X., Ai, S. H. and Shih, C. H., 1988, "Relationship Between Fractal Dimension and Fatigue Threshold Value in Dual-Phase Steels," *Scripta Metallurgica*, Vol. 22, pp. 827~832.
- Williford, R. E., 1988, "Scaling Similarities between Fracture Surfaces, Energies, and a Structure Parameter," *Scripta Metallurgica*, Vol. 22, pp. 197~200.